

Grape ripening as a past climate indicator

Summer temperature variations are reconstructed from harvest dates since 1370.

French records of grape-harvest dates in Burgundy were used to reconstruct spring–summer temperatures from 1370 to 2003 using a process-based phenology model developed for the Pinot Noir grape. Our results reveal that temperatures as high as those reached in the 1990s have occurred several times in Burgundy since 1370. However, the summer of 2003 appears to have been extraordinary, with temperatures that were probably higher than in any other year since 1370.

Biological and documentary proxy records have been widely used to reconstruct temperature variations to assess the exceptional character of recent climate fluctuations^{1–3}. Grape-harvest dates, which are tightly related to temperature, have been recorded locally for centuries in many European countries. These dates may therefore provide one of the longest uninterrupted

series of regional temperature anomalies (highs and lows) without chronological uncertainties¹.

In Burgundy, these officially decreed dates have been carefully registered in parish and municipal archives since at least the early thirteenth century. We used a corrected and updated harvest-date series⁴ from Burgundy, covering the years from 1370 to 2003, to reconstruct spring–summer temperature anomalies that had occurred in eastern France. To convert historical observations into temperature anomalies, we used a process-based phenology model for Pinot Noir, the main variety of grape that has been continuously grown in Burgundy since at least the fourteenth century³ (for details, see supplementary information).

Our yearly reconstruction is significantly correlated (Table 1) with summer temperatures deduced from tree rings in central



A fifteenth-century depiction of the grape harvest from *Les Très Riches Heures du Duc de Berry*, a medieval book of hours.

France⁶ (correlation coefficient, $r=0.53$), the Burgundy part of a spatial multi-proxy reconstruction² ($r=0.69$) and observed summer temperatures in Paris⁷ ($r=0.75$), central England⁸ ($r=0.53$) and the Alps⁹ ($r=0.45$).

Figure 1 shows two early warm decadal fluctuations: one in the 1380s ($+0.72\text{ }^{\circ}\text{C}$) and one in the 1420s ($+0.57\text{ }^{\circ}\text{C}$), both above the 95th percentile. The warm period of the 1420s was followed by a cold period that lasted from the mid-1430s to the end of the 1450s ($-0.45\text{ }^{\circ}\text{C}$, under the 10th percentile). Our series also reveals particularly warm events, above the 90th percentile, in the 1520s and between the 1630s and the 1680s. These decades were as warm as the end of the twentieth century. The high-temperature event of 1680 was followed by a cooling, which culminated in the 1750s (under the 5th percentile) — the start of a long cool period that lasted until the 1970s.

The inferred anomaly for the summer of 2003 represents an unprecedented event. It was $+5.86\text{ }^{\circ}\text{C}$ warmer than the reference period (1960–89), whereas the next highest anomaly during the whole period was $+4.10\text{ }^{\circ}\text{C}$ in 1523. This confirms and refines the conclusions of previous studies^{2,10} about the exceptional warmth of the 2003 summer in France.

Grape-harvest dates offer the potential to trace geographical variations in temperature over large parts of Europe and the Middle East over past centuries. This climate, history and phenology synergy can be used to reconstruct temperatures that will substantially add to the long proxy-record databases and provide insight into regional-scale climate variations.

Isabelle Chuine*, Pascal Yiou†, Nicolas Viovy†, Bernard Seguin‡, Valérie Daux†, Emmanuel Le Roy Ladurie§

Table 1 Linear correlation coefficients between reconstructed temperatures

| Series | Tree rings (JJA) | Multi-proxy (JJA) | Multi-proxy (AMJJA) | Paris (AMJJA) | Central England (AMJJA) | Alps (JJA) |
|--|------------------|-------------------|---------------------|-----------------|-------------------------|-----------------|
| Time range | 1750–1975 | 1500–1998 | 1659–1998 | 1787–2000 | 1663–1992 | 1760–1998 |
| Linear correlation coefficient, r (grape-harvest date) | 0.53 ± 0.09 | 0.57 ± 0.06 | 0.69 ± 0.06 | 0.75 ± 0.07 | 0.53 ± 0.08 | 0.45 ± 0.09 |

Linear correlation coefficients between temperatures reconstructed from grape-harvest dates in Burgundy and other observed or reconstructed temperatures are shown. Comparison with temperatures reconstructed from a tree-ring database⁵ used the closest grid point to Burgundy in the data set. Comparison with multi-proxy reconstructed temperatures² used the four closest grid points to Burgundy in the data set. The Paris⁷, central England⁸, and Alps⁹ series are observed temperatures (instrumental series). Correlations were computed on the common time intervals between two time series. 95% confidence intervals are shown. JJA, June to August; AMJJA, April to August.

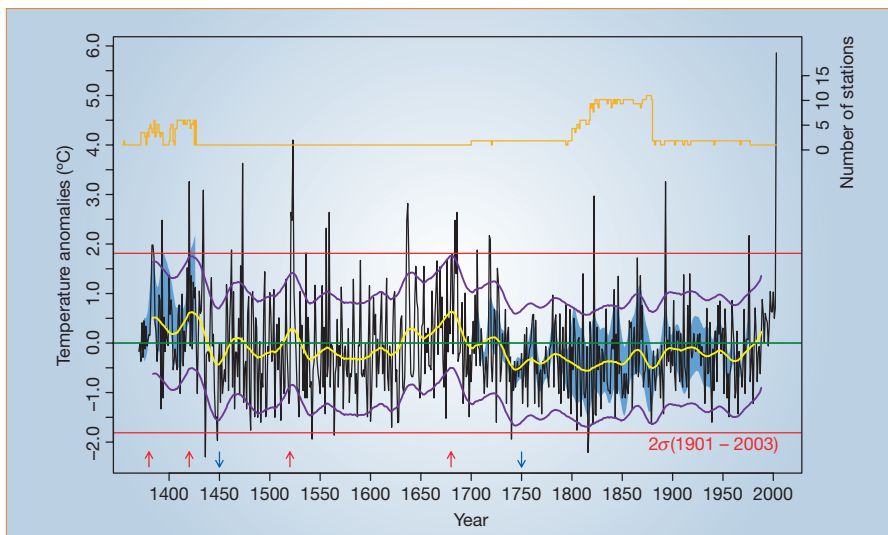


Figure 1 April–August temperature anomalies in Burgundy, France, as reconstructed from grape-harvest dates from 1370 to 2003. Yearly anomalies are in black and the 30-year gaussian filter is in yellow. Confidence intervals due to vineyard differences, with an 11-year smoothing, are shaded in blue; these are estimated from the inter-station variability upper 90th and lower 10th percentiles, and are determined when there are more than three available observations in a year. Orange line (number of stations) represents the number of observed harvest dates for each year, indicating where the confidence intervals are computed. Confidence intervals with two s.e., due to the regression between observed and reconstructed temperature in Dijon, are in purple. These were obtained by regressing the reconstructed temperature with the observed temperature over 1880–2000. Green horizontal (zero) line is determined from the 1960–89 reference period. Red horizontal lines represent the 2σ interval of the reconstructed temperature for the twentieth century (1901–2003). Vertical arrows indicate warm decadal periods (red) above the 90th percentile and the cold trends (blue) under the 10th percentile.

*CEFE-CNRS, 1919 route de Mende, 34293 Montpellier, France

†LSC-CEA-CNRS CE Saclay l'Orme des Merisiers, 91191 Gif-sur-Yvette, France
e-mail: pascal.yiou@cea.fr

‡INRA Site Agroparc, domaine Saint-Paul, 84914 Avignon Cedex 9, France

§Collège de France, 75231 Paris Cedex 05, France

1. Pfister, C. *Wetternachhersage. 500 Jahre Klimavariationen und Naturkatastrophen 1496–1995* (Haupt, Bern, Stuttgart and Wien, 1999).
2. Luterbacher, J., Dietrich, D., Xoplaki, E., Grosjean, M. & Wanner, H. *Science* **303**, 1499–1503 (2004).
3. Jones, P. D. & Mann, M. E. *Rev. Geophys.* **42**, doi:10.1029/2003RG000143 (2004).
4. Le Roy Ladurie, E. *Histoire du Climat depuis l'An Mil* (Champs Flammarion, Paris, 1983).
5. Robinson, J., Dinsmoor, A. & Smart, R. E. *The Oxford Companion to Wine* (Oxford University Press, 1999).
6. Briffa, K. R., Jones, P. D. & Schweingruber, F. H. *Quat. Res.* **30**, 36–52 (1988).
7. Renou, E. *Ann. Bur. Centr. Météorol.* **B 195–226** (1887).
8. Manley, G. Q. *J. R. Meteorol. Soc.* **100**, 389–405 (1974).
9. Boehm, R. *et al. Int. J. Climatol.* **21**, 1779–1801 (2001).
10. Schär, C. *et al. Nature* **427**, 332–336 (2004).

Supplementary information accompanies this communication on Nature's website.

Competing financial interests: declared none.

Climate

Large-scale warming is not urban

Controversy has persisted^{1,2} over the influence of urban warming on reported large-scale surface-air temperature trends. Urban heat islands occur mainly at night and are reduced in windy conditions³. Here we show that, globally, temperatures over land have risen as much on windy nights as on calm nights, indicating that the observed overall warming is not a consequence of urban development.

Observations of the minimum temperature (T_{\min}) over 24 hours at 264 stations worldwide since 1950 were expressed as anomalies, relative to the period 1961–90 where possible. Coverage of T_{\min} data was good north of 20° N, in Australasia and in the western tropical Pacific, but poor in Africa, South America, Antarctica and parts of southern Asia. Reanalysed⁴ daily-average near-surface wind components were used to classify the T_{\min} anomalies into 'windy' (upper tercile) and 'calm' (lower tercile) conditions. Daily average wind speeds were used because the timings of temperature extremes are not known. For stations between 140° E and the dateline, T_{\min} — which occurs most frequently in the early morning — was matched with the previous day's speed. This is because the early morning in terms of universal time (equivalent to Greenwich Mean Time) is still in the previous day in the Far East.

Annual and seasonal anomalies of T_{\min} were gridded on a 5° × 5° resolution for windy, calm and 'all' conditions. Coverage was at least 200 grid boxes (equivalent to

more than 27% of global land area) in 1958–99. For 1950–2000, the trends of global annual average T_{\min} for windy, calm and all conditions were identical (0.19 ± 0.06 °C per decade; Fig. 1a). So, urbanization has not systematically exaggerated the observed global warming trends in T_{\min} . The same can be said for poor instrumental exposure and microclimatic effects, which are also reduced when instruments are well ventilated⁵.

When the criterion for 'calm' was changed to the lightest decile of wind strength, the global trend in T_{\min} was unchanged. The analysis is therefore robust to the criterion for 'calm'. To assess the effect of time differences between the reanalysis⁴ daily-average winds and T_{\min} , I repeated the analysis using 26 stations in North America and Siberia that have hourly or six-hourly reports of simultaneous temperature and wind. Again, windy and calm nights warmed at the same rate, in this case by 0.20 °C per decade.

Because a small sample was used, I compared global trends for the reduced period 1950–93 with published all-conditions trends for that period based on a sample of over 5,000 stations⁶. All differences were within ± 0.02 °C per decade. This robustness arises because of the spatial coherence of surface temperature variations and trends⁷.

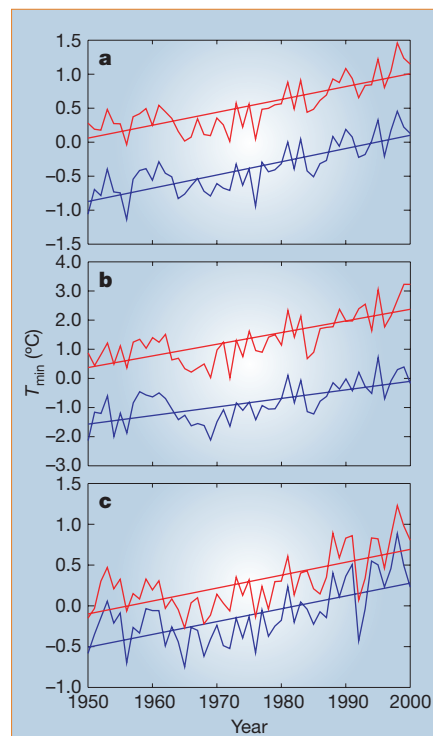


Figure 1 Anomalies in T_{\min} for windy (red) and calm (blue) conditions. **a**, Annual global data; **b**, winter data (December to February) for Northern Hemisphere land north of 20° N; **c**, summer data (June to August) for Northern Hemisphere land north of 20° N. The linear trend fits, and the $\pm 2\sigma$ error ranges given in the text, were estimated by restricted maximum likelihood¹⁰, taking into account autocorrelation in the residuals. As expected from the reduced stratification of the boundary layer, T_{\min} is, on average, warmer on windy nights than on calm nights.

The global annual result conceals a relative warming of windy nights in winter in the extratropical Northern Hemisphere (Fig. 1b), mainly in western Eurasia. The observed tendency to an increased positive phase of the North Atlantic Oscillation⁸ implies that the windier days in western Eurasia had increased warm advection from the ocean⁹, yielding greater warming. In summer in the extratropical Northern Hemisphere (Fig. 1c), there was no relative change in T_{\min} on windy nights. At that time of year, atmospheric circulation changes are less influential, but an urban warming signal is still absent. In the tropics, calm nights warmed relative to windy nights on an annual average, but only by 0.02 ± 0.01 °C per decade, which is much less than the overall tropical warming in T_{\min} (0.16 ± 0.03 °C).

This analysis demonstrates that urban warming has not introduced significant biases into estimates of recent global warming. The reality and magnitude of global-scale warming is supported by the near-equality of temperature trends on windy nights with trends based on all data.

David E. Parker

Hadley Centre, Meteorological Office,
Exeter EX1 3PB, UK

e-mail: david.parker@metoffice.com

1. Kalnay, E. & Cai, M. *Nature* **423**, 528–531 (2003).
2. Peterson, T. C. *J. Clim.* **16**, 2941–2959 (2003).
3. Johnson, G. T. *et al. Bound. Layer Meteorol.* **56**, 275–294 (1991).
4. Kalnay, E. *et al. Bull. Am. Meteorol. Soc.* **77**, 437–471 (1996).
5. Parker, D. E. *Int. J. Climatol.* **14**, 1–31 (1994).
6. Easterling, D. R. *et al. Science* **277**, 364–367 (1997).
7. Jones, P. D., Osborn, T. J. & Briffa, K. R. *J. Clim.* **10**, 2548–2568 (1997).
8. Folland, C. K. *et al. in Climate Change 2001: The Scientific Basis. Contribution of Working Group I to the Third Assessment Report of the Intergovernmental Panel on Climate Change* (eds Houghton, J. T. *et al.*) 99–181 (Cambridge Univ. Press, Cambridge, UK, 2001).
9. Hurrell, J. W. & van Loon, H. *Climat. Change* **36**, 301–326 (1997).
10. Digggle, P. J., Liang, K. Y. & Zeger, S. L. *Analysis of Longitudinal Data* (Clarendon, Oxford, 1999).

Competing financial interests: declared none.

Atmospheric science

Early peak in Antarctic oscillation index

The principal extratropical atmospheric circulation mode in the Southern Hemisphere, the Antarctic oscillation (or Southern Hemisphere annular mode), represents fluctuations in the strength of the circumpolar vortex and has shown a trend towards a positive index in austral summer in recent decades, which has been linked to stratospheric ozone depletion^{1,2} and to increased atmospheric greenhouse-gas concentrations^{3,4}. Here we reconstruct the austral summer (December–January) Antarctic oscillation index from sea-level pressure measurements over the twentieth century⁵ and find that large positive values, and positive trends of a similar magnitude